

# Effects of Calcination Temperature and A/B Ratio on the Dielectric Properties of (Ba,Ca)(Ti,Zr,Mn)O<sub>3</sub> for Multilayer Ceramic Capacitors with Nickel Electrodes

Wen-Hsi Lee\* and T. Y. Tseng\*

Department of Electronics Engineering, National Chiao-Tung University, Hsinchu, Taiwan

Detlev F. K. Hennings\*

Philips Research Laboratories, 52066 Aachen, Germany

The electrical performance of multilayer ceramic capacitors (MLCCs) with Ni inner electrodes, made from (Ba,Ca)-(Ti,Zr,Mn)O<sub>3</sub> (BCTZM), is closely related to the calcination temperature and the A/B ratio of the powder. For materials showing A/B = 1.000, the lifetime, the breakdown voltage, and the RC increase with higher calcination temperatures. No significant effect of the calcination temperature on RC and lifetime was found for materials showing A/B = 0.991. The isoelectric point of BCTZM is shifted toward higher pH values when the calcination temperature is decreased. The above results are attributed to the colloidal stability of aqueous BCTZM suspensions and the resulting green density of powder compacts.

## I. Introduction

(Ba,Ca)(Ti,Zr,Mn)O<sub>3</sub> (BCTZM) is commonly used as a basic material for multilayer ceramic capacitors (MLCCs) with the temperature specification Y5V. Ca and Zr are employed for broadening and shifting the dielectric maximum at the Curie point ( $T_C$ ) to room temperature. Mn is used as a strong acceptor for trapping conduction electrons, when MLCCs are cofired with Ni base metal electrodes (BMEs) in reducing atmosphere. A previous report by Sumita *et al.*<sup>1</sup> stresses the influence of the calcination temperature of BCTZM on the lifetime stability. They claimed that calcination at higher temperatures significantly improves the lifetime of MLCCs.

The fundamental reason for the calcination effect on the lifetime is not yet fully understood. The present work deals with the influence of small changes of the A/B ratio and the calcination temperature on the microstructure and lifetime stability of MLCCs prepared from BCTZM.

## II. Experimental Procedure

The experimental material BCTZM with the standard composition (Ba<sub>0.86</sub>Ca<sub>0.14</sub>)(Ti<sub>0.85</sub>Zr<sub>0.14</sub>Mn<sub>0.01</sub>)O<sub>3</sub> was prepared from reagent-grade BaCO<sub>3</sub>, CaCO<sub>3</sub>, TiO<sub>2</sub>, ZrO<sub>2</sub>, and MnCO<sub>3</sub>. Mn was incorporated on the B-sites, according to the observed<sup>2</sup> solubility of Mn on B-sites of >1.5 mol%. Materials showing two different atomic ratios of A-site ions (Ba, Ca) and B-site ions (Ti, Zr, Mn) have been prepared: material I, A/B = 1.000 ± 0.0015; material II, A/B = 0.991 ± 0.0015. The A/B ratio was carefully fixed by analytical means (XRF). The raw materials were mixed in aqueous

suspension in a ball-mill, using Y-stabilized zirconia balls of 2 mm diameter. The powder mixtures were calcined for 12 h in air at 900°, 1000°, 1100°, and 1200°C in air.

For manufacturing of green MLCC chips a water-based tape casting technique was employed. For slurry preparation the calcined powder was milled to a particle size of  $d_{50} = 1.0 \mu\text{m}$  and mixed with PVA binder solution, dispersant, defoamer agent, plasticizer, and water. Dielectric layers were printed with a Ni electrode pattern and stacked under appropriate pressure (210 bar) and heat. Green chips of size “0805” (EIA Code 0.08 in. × 0.05 in.) with 20 dielectric layers of 15  $\mu\text{m}$  (sintered thickness) were formed by cutting. Binder burnout was carried out at 250°C for 10 h. MLCCs were fired at 1300°C for 2 h in a reducing atmosphere of moist nitrogen and hydrogen, having an oxygen partial pressure of  $\approx 10^{-14}$  bar. After sintering, the MLCCs were annealed for re-oxidation at 900–1200°C in N<sub>2</sub>/O<sub>2</sub> having an oxygen partial pressure of  $\approx 10^{-4}$  bar. The copper terminations were dipped and fired at 850°–900°C at an oxygen partial pressure of  $\approx 10^{-4}$  bar. The microstructure of sintered samples was examined by scanning electron microscopy (SEM; Hitachi Model S2500). The capacitance and the dissipation factor were measured at 1 kHz/0.5 V<sub>rms</sub>, using an HP 4194A bridge. The insulation resistance (IR) was determined after applying 50 V for 60 s. The lifetime stability of the dielectric material was ascertained by means of highly accelerated lifetime tests (HALT) at 140°C and 300 V (20 V/ $\mu\text{m}$ ).

Dispersions for micro-electrophoresis were prepared by mixing about 0.01 g of each BCTZM powder to give a concentration of 10<sup>-3</sup> mol/L H<sub>2</sub>O, using an ultrasonic bath. The pH of the dispersions was adjusted by adding a few drops of either 0.01M HCl or NaOH followed by thorough mixing. The zeta potential of the BCTZM powder was measured as a function of pH, using a commercial Lazer Zee Meter. Ammonium polyacrylate with a molecular weight of about 4000 was used to disperse BCTZM ceramic powder in water. Sedimentation of BCTZM slurries was studied as a function of the calcination temperature. Before sedimentation tubes were filled, the slurries were milled in an attritor for 2 h. All tubes were filled at the same level and all slurries contained the same amount of ceramic powder (solid content 60 wt%) and 0.8 wt% ammonium polyacrylate dispersant (DISPEX-A, Allied Colloids, Hamburg, Germany). The sedimentation levels were measured when they did not change any more (i.e., after a few days). The green density was determined from the ratio of weight and volume and the fired density by means of the Archimedes method.

## III. Results and Discussion

### (I) XRD Studies

X-ray diffraction (XRD) revealed BaCO<sub>3</sub> second phase in all BCTZM powders calcined at temperatures <1100°C, independent

W. Huebner—contributing editor

Manuscript No. 189594. Received January 28, 1999; approved December 1, 1999.  
\*Member, American Ceramic Society.

**Table I.** Effect of Calcination Temperature on the Electrical Properties of BCTZM MLCCs<sup>†</sup>

| $T_{\text{calcin.}} (^{\circ}\text{C})$ | A/B = 1.000      |                                   |                                |              | A/B = 0.991      |                                   |                                |              |
|---|------------------|-----------------------------------|--------------------------------|--------------|------------------|-----------------------------------|--------------------------------|--------------|
|   | $K_{\text{max}}$ | $T_{\text{C}} (^{\circ}\text{C})$ | IR ( $\times 10^{10} \Omega$ ) | HALT (ave h) | $K_{\text{max}}$ | $T_{\text{C}} (^{\circ}\text{C})$ | IR ( $\times 10^{10} \Omega$ ) | HALT (ave h) |
| 900                                     | 7850             | 16                                | 26.2                           | 7.4          | 8900             | 45                                | 16.2                           | 6.9          |
| 1000                                    | 8100             | 15                                | 28.6                           | 8.6          | 8500             | 45                                | 14.8                           | 7.2          |
| 1100                                    | 8300             | 12                                | 30.9                           | 10.0         | 9400             | 45                                | 14.5                           | 7.4          |
| 1200                                    | 9100             | 11                                | 32.4                           | 11.6         | 10500            | 45                                | 14.2                           | 7.1          |

<sup>†</sup>Twenty dielectric layers of 15  $\mu\text{m}$ ; highly accelerated lifetime test (HALT) at  $E = 20 \text{ V}/\mu\text{m}$  and  $140^{\circ}\text{C}$ .

of the A/B ratio. The estimated detection limit of BaCO<sub>3</sub> was  $\approx 1$  mol%. While the BaCO<sub>3</sub> peak was almost identical for A/B = 1.000 and A/B = 0.991 after calcination at  $900^{\circ}\text{C}$ , it became weaker at  $1000^{\circ}\text{C}$  for A/B = 0.991. All powders calcined at temperatures  $> 1100^{\circ}\text{C}$  no longer showed peaks of BaCO<sub>3</sub> second phase.

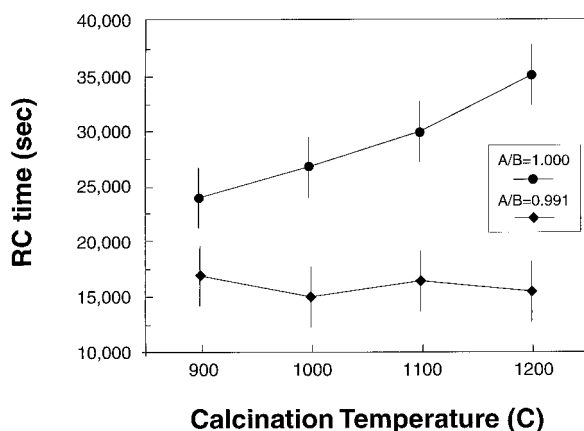
## (2) Electrical Properties

Table I shows the measured values of the maximum dielectric constant ( $K_{\text{max}}$ ) at the Curie point ( $T_{\text{C}}$ ), the insulation resistance (IR), and the average lifetime under HALT stress for A/B = 1.000 and 0.991 and calcination temperatures in the range  $900^{\circ}$  to  $1200^{\circ}\text{C}$ .  $K_{\text{max}}$  was found to increase for both A/B ratios with higher calcination temperatures. Significant changes of  $T_{\text{C}}$ , IR, and HALT were observed only for A/B = 1.000 with increasing calcination temperature. A remarkable effect was the large scatter of RC and lifetimes observed in HALT of MLCCs showing A/B = 1.000. MLCCs of materials with A/B = 0.991 showed in contrast much smaller scatter of IR and lifetime. This result is in full agreement with that of Sumita,<sup>1</sup> who studied BaTiO<sub>3</sub> with Ba excess. However, it is important to note that the lifetime is obviously independent of the calcination temperature for A/B = 0.991, i.e., for A/B < 1.

The influence of the calcination temperature on RC and the breakdown voltage,  $V_{\text{bd}}$ , is shown in Figs. 1 and 2. For A/B = 1.000, RC and  $V_{\text{bd}}$  gradually increased with increasing calcination temperature, while for A/B = 0.991 the calcination temperature had only little influence. Once again, the results of RC and  $V_{\text{bd}}$  illustrate the different influence of the calcination temperature on materials showing A/B = 1.000 and A/B = 0.991. These results confirm earlier observations<sup>3</sup> that the effect of the calcination temperature on the electrical properties is different even for small changes of the A/B ratio.

## (3) Microstructure Examination

Figures 3 and 4 show the influence of the calcination temperature on the microstructure of MLCCs prepared from materials showing different A/B ratios of 1.000 and 0.991. Samples with



**Fig. 1.** RC time as a function of calcination temperature for BCTZM with A/B =  $1.000 \pm 0.0015$  and A/B =  $0.991 \pm 0.0015$ , sintered at  $1300^{\circ}\text{C}$  in 99/1 N<sub>2</sub>/H<sub>2</sub> at  $p_{\text{O}_2} \approx 10^{-14}$  bar.

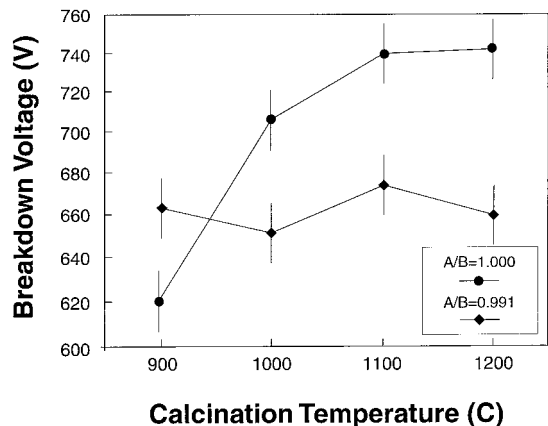


**Fig. 2.** Breakdown voltage ( $V_{\text{bd}}$ ) as a function of calcination temperature for BCTZM with A/B =  $1.000 \pm 0.0015$  and A/B =  $0.991 \pm 0.0015$ , sintered at  $1300^{\circ}\text{C}$  in 99/1 N<sub>2</sub>/H<sub>2</sub> at  $p_{\text{O}_2} \approx 10^{-14}$  bar.

A/B = 1.000 (Fig. 3) exhibited a smaller grain size than those of materials with A/B = 0.991 (Fig. 4). In contrast to A/B = 1.000, no significant influence of the calcination temperatures on the grain size was observed for A/B = 0.991, although the grains were remarkably larger. Waser<sup>4</sup> reported that BaTiO<sub>3</sub>-based compositions with A/B < 1 exhibit a stronger trend to degradation than those showing A/B > 1. Since the Ti-rich second-phase Ba<sub>6</sub>Ti<sub>17</sub>O<sub>40</sub> was found to be stable toward degradation,<sup>5</sup> our results should be interpreted in the light of grain size effects.<sup>6</sup> This interpretation offers a plausible explanation of the influence of the calcination temperature on the lifetime of BCTZM with different A/B ratios. Corresponding to the larger grain size, the lifetime of samples showing A/B = 0.991 should be shorter than that of A/B = 1.000. In the case of A/B = 0.991 no significant influence of the calcination temperature on the grain size as well as on the lifetime of MLCCs was observed. The large scatter of lifetime and IR observed in MLCCs with A/B = 1.000 may be explained in terms of the broader grain size distribution observed in these samples (Fig. 3).

The observation of the microstructure gives a more consistent picture of the influence of the calcination temperature on the electrical properties of MLCCs, showing different A/B ratios of 1.000 and 0.991. However, the different effect of the calcination temperature on the microstructures of both series it is not yet understood.

## (4) Zeta Potential and Sedimentation Measurement

The electrophoretic mobility of BCTZM powders, showing A/B = 1.000 and A/B = 0.991, was studied as a function of pH to determine the isoelectric points (IEPs). Figure 5 shows for A/B = 1.000 a gradual increase of the IEP from pH 7.5 to pH 10.0 after decrease of the calcination temperature from  $1200^{\circ}$  to  $900^{\circ}\text{C}$ . For A/B = 0.991 only a shift of the IEP from pH 7.5 to 8.5 was observed.

The zeta potential of BCTZM with A/B = 1.000 was generally found smaller than that of A/B = 0.991. A different dispersion behavior can be thus expected for BCTZM powders showing different A/B ratios and calcination temperatures.

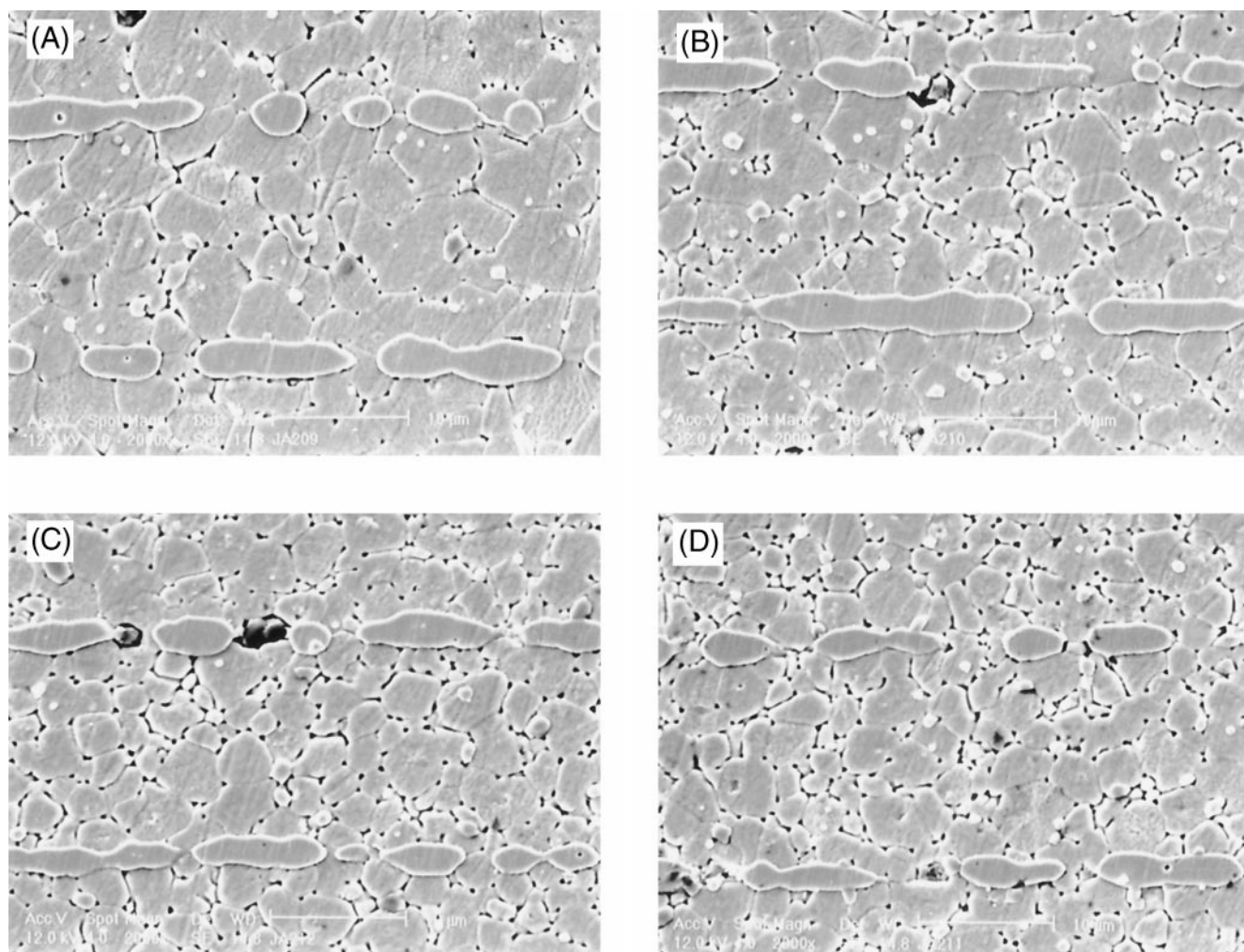


**Fig. 3.** Microstructure of MLCCs of BCTZM showing  $A/B = 1.000 \pm 0.0015$ , calcined at 900° (A), 1000° (B), 1100° (C), and 1200°C (D); cofired for 2 h with Ni electrode at 1300°C in 99/1  $N_2/H_2$  at  $p_{O_2} \approx 10^{-14}$  bar.

The colloidal stability of BCTZM powder dispersions could be ascertained by sedimentation experiments, using a solution of ammonium polyacrylate as dispersant which had a molecular weight of 4000. For these experiments powder suspensions showing a solid content of 60 wt% were used to fill tubes of 50 cm length. The dispersant concentration must not exceed a certain limit, because otherwise destabilization occurs, due to electric double layer compression<sup>7</sup> by electrolytic species in the solution. Therefore, a dispersant concentration of 0.8 wt% was chosen in our experiments. Samples calcined at lower temperature showed the most rapid setting. The powder with  $A/B = 1.000$  calcined at 900°C typically accomplished sedimentation within 30 min, while samples calcined at higher temperature did not exhibit significant sedimentation in this time. Increasing sedimentation times, i.e., stabilization of the slurry, were observed for both B/A ratios with increasing calcination temperature.

Figure 6 depicts the measured sedimentation heights of BCTZM slurries as a function of the calcination temperature. The sedimentation volume decreased with increasing calcination temperature. BCTZM powders showing  $A/B = 0.991$ , however, always had the highest packing density. The most stable dispersion also had the smallest sedimentation volume and thus the highest particle packing density.

##### (5) Green Density and Fired Density

MLCC dummies were fired (without electrodes) for 2 h at 1300°C in a moist atmosphere of 99/1  $N_2/H_2$ . The green and fired densities of these dummies were plotted as a function of the calcination temperature in Figs. 7 and 8. For materials showing

$A/B = 1.000$  the green and fired densities both increased with the calcination temperature, while in the case of  $A/B = 0.991$  only the green density was influenced by the calcination temperature. Thus, for  $A/B = 0.991$  the final density can be considered as almost independent of the green density.

The  $A/B$  ratio critically influences the development of the microstructure of  $BaTiO_3$ -based dielectrics. Small excess of  $TiO_2$  leads to formation of  $Ba_6Ti_{17}O_{40}$  second phase.<sup>8</sup> The liquid eutectic  $BaTiO_3$ - $Ba_6Ti_{17}O_{40}$  affects the sintering behavior and enhances grain growth,<sup>9,10</sup> as can be seen in Fig. 4 by the larger grain size of MLCCs with  $A/B = 0.991$ . In the case of  $A/B = 1.000 \pm 0.0015$  negligible amounts of eutectic melt are present, so that a low green density also leads to a low fired density.<sup>11</sup>

The densification rates of BCTZM with  $A/B = 1.000$  and  $A/B = 0.991$ , calcined at various temperatures, were found to be quite different (Figs. 9 and 10). For  $A/B = 1.000$  the maximum shrinkage rate shifts to lower temperatures with increasing calcination temperature. Thus, for calcination at 900°C the maximum shrinkage rate lies at 1300°C, while for a calcination temperature of 1200°C the maximum shrinkage rate is at 1180°C. For Ti-rich powders showing  $A/B = 0.991$  the maximum shrinkage is almost independent of the calcination at  $\approx 1180^\circ C$ . This effect can be considered as characteristic of a liquid-phase sintering mechanism.

## IV. Conclusions

The conclusions drawn from the experimental results are as follows:

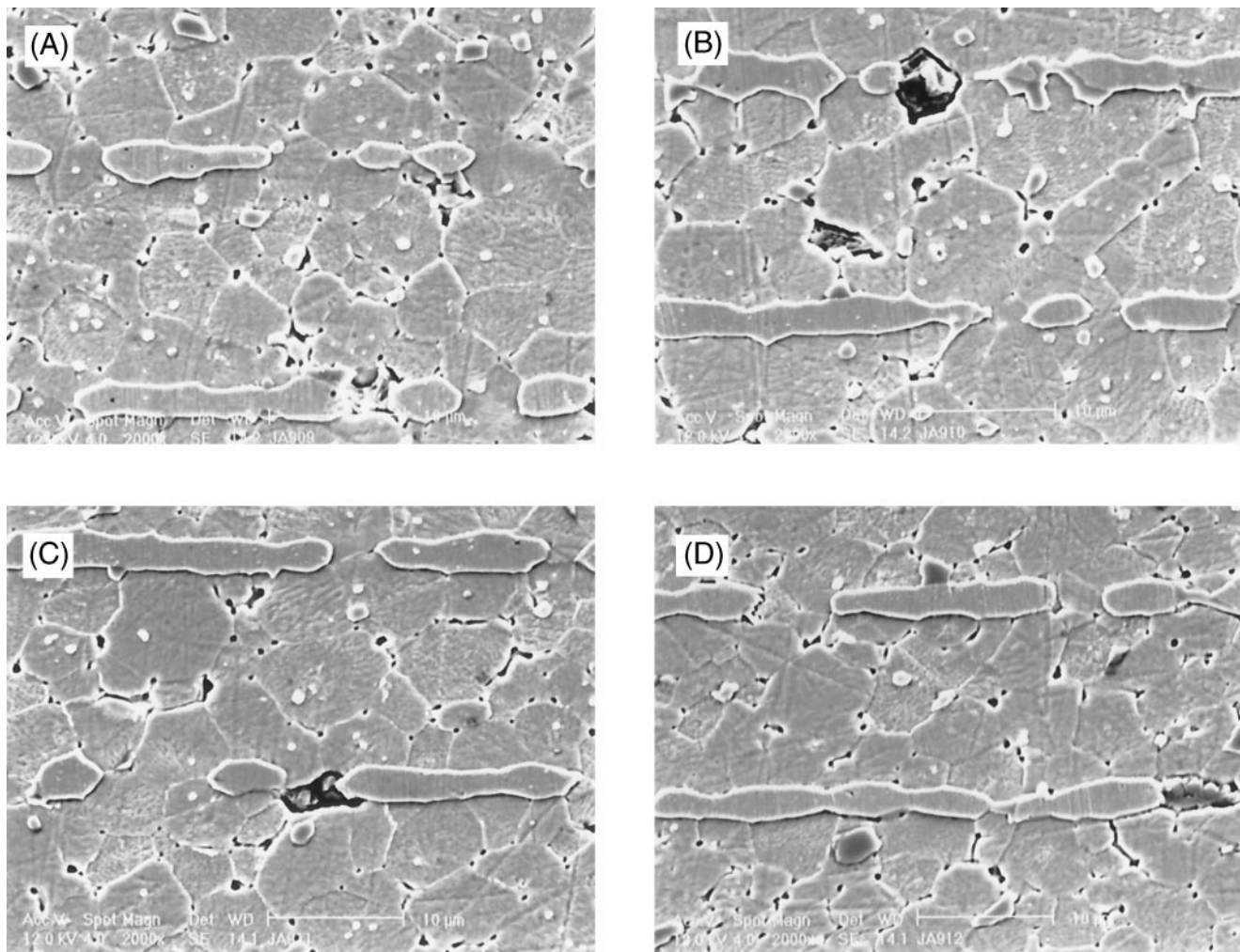


**Fig. 4.** Microstructure of BCTZM with  $A/B = 0.991 \pm 0.0015$ , calcined at 900° (A), 1000° (B), 1100° (C), and 1200°C (D) and cofired for 2 h with Ni electrodes at 1300°C in 99/1 N<sub>2</sub>/H<sub>2</sub> at  $p_{O_2} \approx 10^{-14}$  bar.

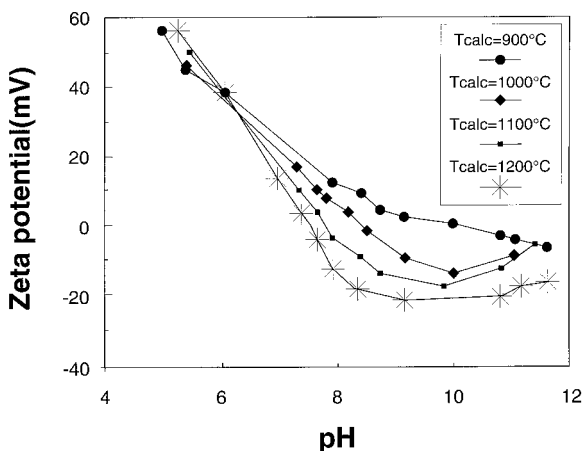


**Fig. 5.** Electrophoretic mobility as function of pH at various calcination temperatures for BCTZM with  $A/B = 1.000 \pm 0.0015$ .

- The effect of calcination temperature on RC, breakdown voltages ( $V_{bd}$ ), and lifetime was observed only in BCTZM showing  $A/B = 1.000 \pm 0.0015$ , forming none or negligible amounts of liquid phase during sintering.
- In materials forming liquid eutectic phase ( $A/B = 0.991 \pm 0.0015$ ), the calcination temperature has a minor effect on RC,  $V_{bd}$ , and lifetime.

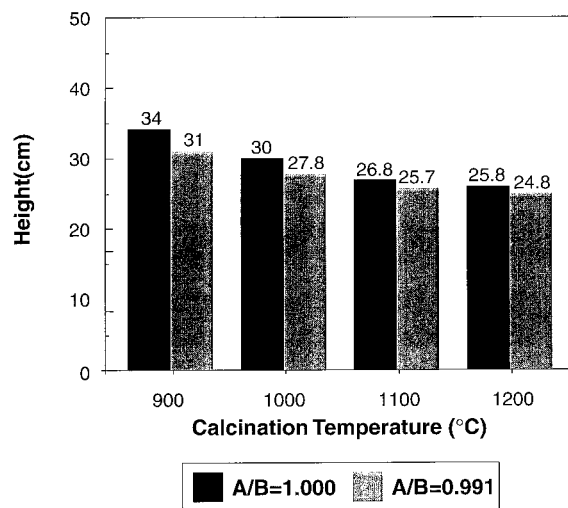


**Fig. 6.** Comparison of the sedimentation height of aqueous BCTZM slurries, containing 0.8 wt% ammonium polyacrylate dispersant, for  $A/B = 1.000 \pm 0.0015$  and  $A/B = 0.991 \pm 0.0015$  at various calcination temperatures.

- In materials forming no liquid eutectic phase ( $A/B = 1.000$ ), the final density, RC,  $V_{bd}$ , and lifetime are closely related to the green density.
- The green density is attributed to the colloidal stability of BCTZM powder dispersions. The colloidal stability of BCTZM

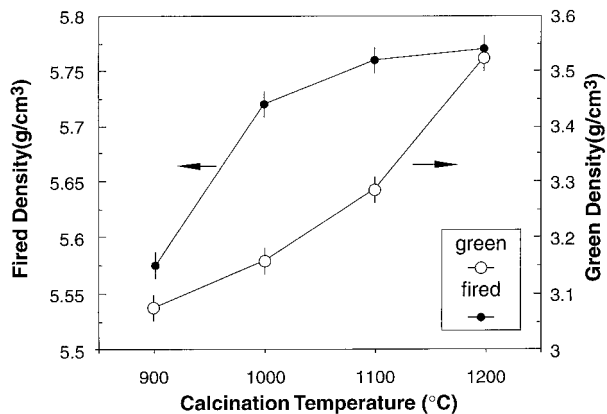


Fig. 7. Green and fired densities as a function of calcination temperature for BCTZM with  $A/B = 1.000 \pm 0.0015$ .

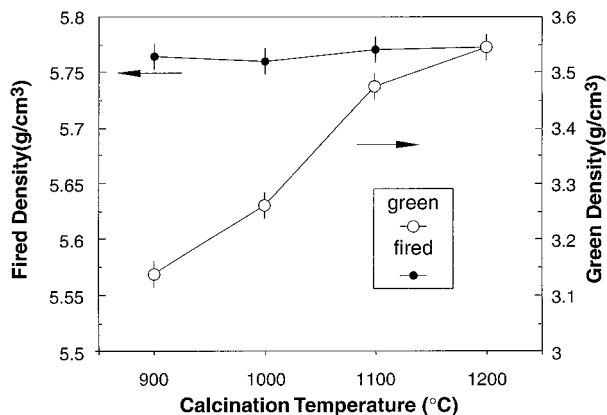


Fig. 8. Green and fired densities as a function of calcination temperature for BCTZM with  $A/B = 0.991 \pm 0.0015$ .

and the density of powder packing in aqueous dispersions increase with the calcination temperature.

• The green density is of minor importance for the final density and electrical performance of materials, forming  $TiO_2$ -rich liquid eutectic phase during sintering ( $A/B = 0.991$ ).

## References

- <sup>1</sup>S. Sumita and T. Nomura, "Effects of Calcination on Lifetime of  $BaTiO_3$ -based Multilayer Ceramic Chip Capacitor with Nickel Electrodes," *Int. J. Soc. Mater. Eng. Resources*, **5** [1] 91–104 (1997).
- <sup>2</sup>D. Hennings, K. Albertsen, P. Hansen, and O. Steigelmann, "Donor–Acceptor Charge Complex Formation in Barium Titanate Ceramics"; pp. 41–51 in *Ceramic Transactions*, Vol. 97, *Multilayer Electronic Ceramic Devices*. Edited by J.-H. Jean, T. K. Gupta, K. M. Nair, and K. Niwa. American Ceramic Society, Westerville, OH, 1999.
- <sup>3</sup>Y. Sakabe, K. Minai, and K. Wakino, "High-Dielectric Constant Ceramic for Base Metal Monolithic Capacitor," *Jpn. J. Appl. Phys. Suppl.* 20-4, **20**, 147–50 (1981).

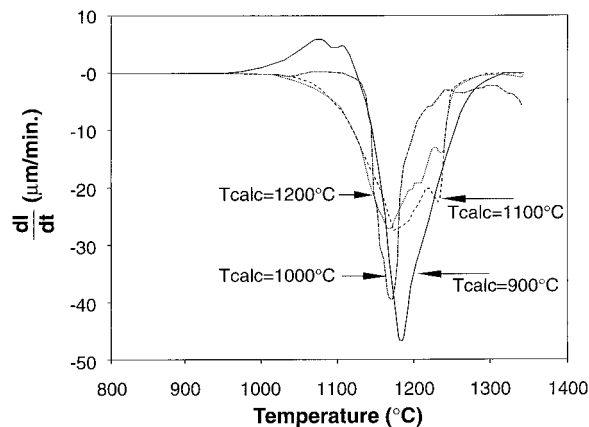


Fig. 9. Densification rate of BCTZM with  $A/B = 0.991 \pm 0.0015$ , calcined at various temperatures.

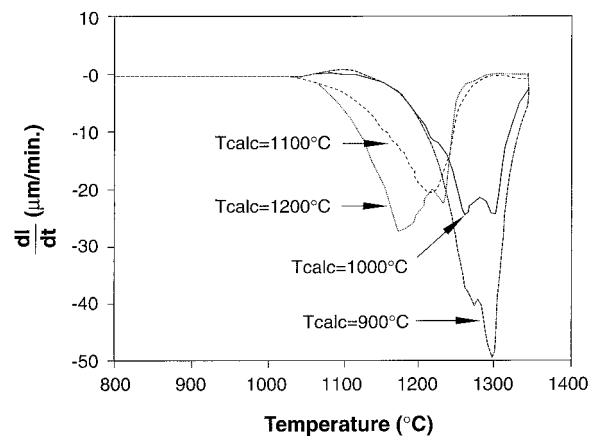


Fig. 10. Densification rate of BCTZM with  $A/B = 1.000 \pm 0.0015$ , calcined at various temperatures.

<sup>4</sup>R. Waser, T. Baiatu, and K. H. Härdtl, "DC Electrical Degradation of Perovskite-Type Titanates," *J. Am. Ceram. Soc.*, **73** [6] 1645–53 (1990).

<sup>5</sup>M. P. Harmer, Y. H. Hu, M. Lal, and D. M. Smyth, "The Effect of Composition and Microstructure on Electrical Degradation in  $BaTiO_3$ ," *Ferroelectrics*, **49**, 71–74 (1983).

<sup>6</sup>H. Neumann and G. Arlt, "Maxwell–Wagner Relaxation and Degradation of  $SrTiO_3$  and  $BaTiO_3$  Ceramics," *Ferroelectrics*, **69**, 179–86 (1986).

<sup>7</sup>R. O. James, "Characterization of Colloids in Aqueous System"; pp. 349–410 in *Advances in Ceramics*, Vol. 21, *Ceramic Powder Science*. American Ceramic Society, Westerville, OH, 1988.

<sup>8</sup>T. Yamamoto, "Influence of Small Ba/Ti Nonstoichiometry on Grain Growth Behaviour in Barium Titanate," *Br. Ceram. Trans.*, **94** [5] 196–200 (1995).

<sup>9</sup>D. F. K. Hennings and R. Janssen, "Control of Liquid Phase Enhanced Grain Growth in Barium Titanate," *J. Am. Ceram. Soc.*, **70**, 23–27 (1987).

<sup>10</sup>D. Hennings, "Liquid Phase Sintering of Barium Titanate," *Ber. Dtsch. Keram. Ges.*, **55** [7] 359–60 (1978).

<sup>11</sup>H.-L. Hsieh and T.-T. Fang, "Effect of Green States on Sintering Behaviour and Microstructure Evolution of High-Purity Barium Titanate," *J. Am. Ceram. Soc.*, **73** [6] 1566–73 (1990). □